

A 69 long non-coding RNA signature predicts relapse and acts as independent prognostic factor in pediatric AML

Tracking no: ADV-2024-012667R1

Zhiyao Ren (Ghent University, Belgium) Jolien Vanhooren (Ghent University, Belgium) Charlotte Derpoorter (Ghent University, Belgium) Barbara De Moerloose (Ghent University Hospital, Belgium) Tim Lammens (Ghent University Hospital, Belgium)

Abstract:

Risk stratification using genetics and minimal residual disease (MRD) has allowed to increase the cure rates of pediatric acute myeloid leukemia (pedAML) up to 70% in contemporary protocols. Nevertheless, approximately 30% of patients still experience relapse, indicating a need to optimize stratification strategies. Recently, long non-coding RNA (lncRNA) expression has been shown to hold prognostic power in multiple cancer types. Here, we aimed at refining relapse prediction in pedAML using lncRNA expression. We built a relapse-related lncRNA prognostic signature, named AMLlnc69, using 871 pedAML patients transcriptomes obtained from the Therapeutically Applicable Research To Generate Effective Treatments (TARGET) repository. We identified a 69 lncRNA signature AMLlnc69 that is highly predictive of relapse-risk (c-index = 0.73), with area under the ROC curve (AUC) values for predicting the 1-, 2-, and 3-year relapse-free survival (RFS) of 0.78, 0.77, and 0.77, respectively. The internal validation using a bootstrap method (resampling times = 1000) resulted in a c-index of 0.72 and AUC values for predicting the 1-, 2-, and 3-year RFS of 0.77, 0.76, and 0.76, respectively. Through a Cox regression analysis, AMLlnc69, NPM mutation and WBC at diagnosis were identified as independent predictors of RFS. Finally, a nomogram was build using these two parameters, showing a c-index of 0.80 and 0.71 after bootstrapping (n =1000). In conclusion, the identified AMLlnc69 will, after prospective validation, add important information to guide management of pedAML patients. The nomogram is a promising tool for easy stratification of patients into a novel scheme of relapse-risk groups.

Conflict of interest: No COI declared

COI notes:

Preprint server: No;

Author contributions and disclosures: Z.R, J.V, and T.L drafted the manuscript. Z.R, J.V and T.L designed the figures. All authors critically revised the manuscript and approved the final version.

Non-author contributions and disclosures: No;

Agreement to Share Publication-Related Data and Data Sharing Statement: The results published here are in whole or part based upon data generated by the Therapeutically Applicable Research to Generate Effective Treatments (<https://www.cancer.gov/ccg/research/genome-sequencing/target>) initiative, phs000218. The data used for this analysis are available at the Genomic Data Commons (<https://portal.gdc.cancer.gov>).

Clinical trial registration information (if any):

1 **A 69 long non-coding RNA signature predicts relapse and acts as independent**
2 **prognostic factor in pediatric AML**

3 Zhiyao Ren^{1,2,3}, Jolien Vanhooren^{1,2,3}, Charlotte Derpoorter^{1,2,3}, Barbara De Moerloose^{1,2,3}, Tim Lammens^{1,2,3}

4
5 ¹ Department of Internal Medicine and Pediatrics, Ghent University, 9000 Ghent, Belgium

6 ² Department of Pediatric Hematology-Oncology and Stem Cell Transplantation, Ghent University Hospital,
7 9000 Ghent, Belgium

8 ³ Cancer Research Institute Ghent, 9000 Ghent, Belgium

9 **Corresponding author**

10 Tim Lammens

11 Department of Pediatric Hematology-Oncology and Stem Cell Transplantation

12 Ghent University Hospital

13 9000 Ghent

14 Belgium

15 E-mail address: Tim.Lammens@UGent.be

16
17 **Running title**

18 LncRNA expression in AML: an independent prognostic factor

19
20 **Key Points**

21 A comprehensive prognostic model of 69 lncRNAs was generated to predict RFS in pedAML and further
22 refining the current risk stratification

23 A nomogram incorporating the 69 lncRNAs signature, NPM mutation and WBC was developed to stratify
24 patients into relapse-risk groups

25
26 **Data sharing statement**

27 The results published here are in whole or part based upon data generated by the Therapeutically Applicable
28 Research to Generate Effective Treatments initiative, phs000218. The data used for this analysis are available at
29 the Genomic Data Commons (<https://portal.gdc.cancer.gov>).

32 Abstract

33 Risk stratification using genetics and minimal residual disease (MRD) has allowed to
34 increase the cure rates of pediatric acute myeloid leukemia (pedAML) up to 70% in
35 contemporary protocols. Nevertheless, approximately 30% of patients still experience relapse,
36 indicating a need to optimize stratification strategies. Recently, long non-coding RNA
37 (lncRNA) expression has been shown to hold prognostic power in multiple cancer types.
38 Here, we aimed at refining relapse prediction in pedAML using lncRNA expression. We built
39 a relapse-related lncRNA prognostic signature, named AML^{lnc69}, using 871 pedAML patients
40 transcriptomes obtained from the Therapeutically Applicable Research To Generate Effective
41 Treatments (TARGET) repository. We identified a 69 lncRNA signature AML^{lnc69} that is
42 highly predictive of relapse-risk (c-index = 0.73), with area under the ROC curve (AUC)
43 values for predicting the 1-, 2-, and 3-year relapse-free survival (RFS) of 0.78, 0.77, and 0.77,
44 respectively. The internal validation using a bootstrap method (resampling times = 1000)
45 resulted in a c-index of 0.72 and AUC values for predicting the 1-, 2-, and 3-year RFS of 0.77,
46 0.76, and 0.76, respectively. Through a Cox regression analysis, AML^{lnc69}, NPM mutation
47 and WBC at diagnosis were identified as independent predictors of RFS. Finally, a
48 nomogram was build using these two parameters, showing a c-index of 0.80 and 0.71 after
49 bootstrapping (n =1000). In conclusion, the identified AML^{lnc69} will, after prospective
50 validation, add important information to guide management of pedAML patients. The
51 nomogram is a promising tool for easy stratification of patients into a novel scheme of
52 relapse-risk groups.

53

54

55

56

57

58

59

60

61

62

63 **Introduction**

64 The 5-year overall survival (OS) rate for pediatric acute myeloid leukemia (pedAML) is now
65 up to 70% with the application of most contemporary protocols¹. This improvement has been
66 achieved through treatment intensification, the optimization of transplant procedures and
67 supportive care, and the introduction of risk-adapted treatment strategies². Risk stratification
68 for pedAML depends mainly on the presence or absence of cytogenetic and molecular
69 abnormalities known to be associated with the achievement of complete remission (CR), OS,
70 and relapse-free survival (RFS)³⁻⁵. The achievement of minimal residual disease (MRD)
71 during treatment has been shown to be another important risk stratification indicator enabling
72 treatment adaptation⁶⁻⁸. Nevertheless, pedAML remains a therapeutic challenge, with high
73 (~30%) relapse rates despite intensive therapy⁹. Relapse is a major cause of pedAML
74 treatment failure and an indicator of poor prognosis¹⁰. Recent coding gene expression
75 analyses revealed the ability of the LSC6 and LSC17 stemness signatures, reflecting the
76 expression of 6 and 17 coding mRNAs, respectively, to predict the event-free survival (EFS)
77 and OS of patients with pedAML^{11,12}. Similarly, the LSC47 signature was developed to
78 predict EFS in the context of existing cytogenetic and molecular risk stratification¹³. Recently,
79 the lncScore, a long non-coding RNA (lncRNA)-based predictor of the EFS and OS of
80 patients with pedAML, was developed¹⁴. However, none of these signatures predicts RFS or
81 has been implemented in a clinical setting. Thus, the further refinement of relapse-based risk
82 stratification for pedAML remains an urgent need.

83

84 LncRNAs are transcripts longer than 200 nucleotides that are not translated into proteins and
85 have highly tissue-specific expression¹⁵. They have been shown to play important roles in
86 normal development and the development of diseases^{16,17}, including pedAML¹⁸. The aberrant

87 expression of key lncRNAs involved in hematopoietic stem cell maintenance and
88 differentiation has been shown to result in the development of hematological
89 malignancies^{19,20}. lncRNA expression also has prognostic power for malignancies such as
90 adult AML²¹, breast cancer²², and neuroblastoma²³. Hence, the inclusion of lncRNA
91 expression in pedAML risk stratification could add value for RFS prediction.

92

93 In this study, we aimed to identify an lncRNA signature that predicts pedAML RFS using
94 publicly available RNA sequencing (RNA-seq) data from patients with pedAML from the
95 Therapeutically Applicable Research to Generate Effective Treatments (TARGET) repository,
96 including cases from Children's Oncology Group (COG) studies AAML0531²⁴ and
97 AAML1031^{25,26}.

98

99 **Methods**

100 **TARGET data acquisition**

101 RNA-seq data and corresponding clinical information on patients with pedAML were
102 retrieved from the TARGET repository (<https://ocg.cancer.gov/programs/target>) and
103 downloaded from the Genomic Data Commons (<https://portal.gdc.cancer.gov>). We included
104 pedAML cases from COG studies AAML0531²⁴ and AAML1031^{25,26}. During enrollment in
105 those clinical trials, which were conducted in accordance with the Declaration of Helsinki,
106 participants provided written informed consent to the use of their data for correlative
107 biological studies. We excluded cases evaluated by low-depth sequencing and sequencing
108 data obtained at non-diagnostic time points, such as after treatment or relapse. As we focused
109 on relapse, only patients whose first event was relapse and those who were censored were
110 included. Patients from the AAML1031 study were allocated to the discovery cohort ($n = 871$)
111 and those from the AAML0531 study were allocated to the validation cohort ($n = 158$;

112 Supplemental Figure 1). Detailed information on each of the included patients is provided in
113 Supplemental Table 1, and the value labels used in Supplemental Table 1 are provided in
114 Supplemental Table 2. Gene annotation was performed using Homo_sapiens.GRCh38.110
115 from the Ensembl project (<http://www.ensembl.org>)²⁷.

116

117 **lncRNA prognostic signature construction**

118 Univariate Cox regression analysis was used to identify lncRNAs associated significantly
119 with RFS ($p < 0.05$). Then, least absolute shrinkage and selection operator (LASSO) Cox
120 regression was used to further filter for lncRNAs associated strongly with RFS, and to
121 estimate their coefficients for linear predictor establishment. During this process, the optimal
122 parameter ' λ ' was obtained through cross-validation to maintain equilibrium between model
123 deviation and variance. The caret, tidyverse, tibble, data.table, survival, survminer, glmnet,
124 pbapply, and magrittr R packages were used for these analyses. Next, an outcome-oriented
125 method was applied using the surv_cutpoint function of the survminer R package to
126 determine an optimal cutoff value that maximized survival differences between low- and
127 high-risk lncRNA signature groups. Finally, the risk score distribution was plotted and RFS
128 status mapping was performed to further analyze the influence of the selected signature on
129 RFS.

130

131 **Outcome analysis and validation**

132 Using the survival and survminer R packages and the Kaplan–Meier (KM) method, RFS and
133 OS probabilities were estimated. Standard errors were calculated using the Greenwood
134 formula, and the data were compared using the log-rank test. Receiver operating
135 characteristic (ROC) curves were drawn and the areas under the curves (AUCs) were
136 calculated using the survminer and timeROC R package to assess model performance at 1, 2,

137 and 3 years. Concordance (c)-indices were calculated for signature assessment using the
138 concordance function²⁸. The bootstrap method, based on 1000-fold resampling, was used for
139 internal validation^{29,30}. Univariate and multivariate Cox regression analyses were performed
140 to obtain independent prognostic values for the lncRNA signature, and c-indices of these
141 values were calculated. Finally, a nomogram was generated using the regplot, survival, rms,
142 ggDCA, and timeROC R packages³¹. The coefficients of lncRNAs in the model generated
143 from discovery cohort data were used for external validation.

144

145 **Comparison of clinical characteristics**

146 Fisher's exact test and the χ^2 test were used to assess distributional differences in categorical
147 data between the low- and high-risk groups. A heatmap of these differences was generated
148 using the ComplexHeatmap R package. The normality of data distributions was assessed
149 using the D'Agostino–Pearson, Anderson–Darling, Shapiro–Wilk, and Kolmogorov–Smirnov
150 tests. Non-normally distributed quantitative data were evaluated using the Mann–Whitney *U*
151 test. Box plots of quantitative results were generated using GraphPad Prism 9.

152

153 **Functional and biological pathway enrichment analyses**

154 Gene set enrichment analysis (GSEA) was performed using the limma, org.Hs.eg.db,
155 clusterProfiler, and enrichplot R packages ($p < 0.05$)³². The hallmark, gene ontology (GO),
156 and Kyoto Encyclopedia of Genes and Genomes (KEGG) gene sets were downloaded from
157 MSigDB (<http://www.broadinstitute.org/msigdb>)³³ and used for this purpose.

158

159 **Results**

160 **Prognostic lncRNA signature establishment**

161 The characteristics of patients in the discovery and validation cohorts are summarized in
162 Supplemental Table 3, and RFS in the two cohorts is illustrated in Supplemental Figure 2.
163 Univariate Cox regression analysis of discovery cohort data yielded 1751 relapse-related
164 lncRNAs (Supplemental Table 4). To improve the prediction accuracy and avoid overfitting,
165 a LASSO Cox regression analysis was performed to construct a linear prognostic model
166 (AML^{lnc69}), in which 69 lncRNAs were retained (Figure 1A, Supplemental Figure 3,
167 Supplemental Table 5.). AML^{lnc69} risk group information, survival data, and expression levels
168 of the lncRNAs used in model construction are provided for all patients in the discovery
169 cohort in Supplemental Table 6. An optimal cutoff value was calculated using the
170 surv_cutpoint function in the survminer R package and an outcome-oriented method that
171 enabled patient assignment to low- and high-risk AML^{lnc69} groups. The risk score distribution
172 is shown in Figure 1B. The RFS status map for all patients with pedAML shows that the
173 proportion of patients with relapse increases with the AML^{lnc69} score (Figure 1C).

174

175 **Signature validation**

176 KM survival curves further illustrated that the RFS rate was significantly lower for high-risk
177 AML^{lnc69} patients than low-risk AML^{lnc69} patients in the discovery cohort (Figure 2A). In
178 addition, the AML^{lnc69} signature was significantly predictive of OS (Figure 2B). To further
179 substantiate the predictive value of the model, we performed ROC analyses with the
180 calculation of AUCs for the prediction of 1-, 2-, and 3-year RFS; these values were 0.78, 0.77,
181 and 0.77, respectively, with a corresponding c-index of 0.73 (Figure 2C). Internal validation
182 yielded a c-index of 0.72 and AUCs for the prediction of 1-, 2-, and 3-year RFS of 0.77, 0.76,
183 and 0.76, respectively (Supplemental Table 7). As some patients underwent hematopoietic
184 stem cell transplantation (HSCT) during their first CR periods, which might confound the
185 survival analysis, separate KM RFS curves were generated for patients who did and did not

186 undergo this procedure. These curves illustrated that the model remains valid irrespective of
187 HSCT performance (Figure 3A, B).

188

189 The potential of the LSC6¹¹, LSC17¹², and LSC47¹³ mRNA signatures and the IncScore¹⁴ for
190 pedAML risk stratification has been demonstrated. As these signatures were generated for the
191 prediction of OS and EFS, we tested their predictive value for RFS in the discovery cohort.
192 Our analyses confirmed this value. KM plots showed that all three models successfully
193 stratified patients based on RFS. However, acceptable AUCs (~0.65) for 1-, 2-, and 3-year
194 RFS prediction were obtained only for the LSC47 signature and IncScore, and these values
195 were significantly lower than those obtained for the AML^{Inc69} (Supplemental Figure 4).

196

197 Next, AML^{Inc69} was validated with an independent validation cohort ($n = 158$ patients with
198 pedAML; Supplemental Figure 1). Patients in the validation cohort were categorized into
199 low- and high-risk groups based on the AML^{Inc69}, yielding AUCs of 0.66, 0.68, and 0.70 for
200 1-, 2-, and 3-year RFS prediction, respectively (Supplemental Figure 5A, B). As the benefit
201 of adding gemtuzumab ozogamicin was a randomized question in this study cohort, we
202 evaluated if AML^{Inc69} was predictive for RFS on each of the randomization arms.
203 Interestingly, KM survival analysis illustrated that AML^{Inc69} remained predictive, irrespective
204 of gemtuzumab ozogamicin randomization arm (Supplemental Figure 5C, D).

205

206 Subsequently, we plotted the distribution of cytogenetic/molecular risk for the AML^{Inc69} low-
207 and high-risk groups in the discovery cohort. Importantly, a significant proportion of
208 conventionally stratified standard-risk patients could be reclassified as high-risk according to
209 the AML^{Inc69} (Figure 3C). Furthermore, KM plots showed that the AML^{Inc69} could be used to
210 reclassify patients in all (low, standard, and high) traditional risk groups based on

211 cytogenetic/molecular characteristics (Figure 3D–F, Supplemental Figure 6). The frequency
212 distributions of patient characteristics according to HSCT administration and AML^{Inc69} risk
213 group are shown in Supplemental Table 8.

214 Altogether, these results illustrated that AML^{Inc69} use could improve traditional
215 cytogenetic/molecular risk stratification, better defining low-risk and high-risk patients in
216 terms of RFS.

217

218 **AML^{Inc69} is an independent prognostic factor**

219 To evaluate whether the AML^{Inc69} is an independent prognostic factor, we first performed
220 Cox regression analysis and calculated c-indices for the discovery cohort. Due to the
221 requirement for complete data, 704 patients were included in this analysis. Univariate Cox
222 regression analysis indicated that age, white blood cell (WBC) count at the time of diagnosis,
223 presence of core binding factor (CBF), KMT2A, t(6;11)(q27;q23), t(9;11)(p22;q23),
224 t(10;11)(p11.2;q23), trisomy 21, nucleophosmin (NPM) mutation, MRD at the end of
225 induction course 1, MRD at end of induction course 2, and the AML^{Inc69} signature were
226 prognostic factors (Figure 4A, Supplemental Table 9). In this analysis, AML^{Inc69} performed
227 well in distinguishing low- and high-risk individuals in all subgroups (defined according to
228 genetics and MRD; Supplemental Figure 7), although some of these subgroups were small (n
229 < 5) and these results should be interpreted with caution. Next, significant variables were
230 examined further in a multivariate Cox analysis, which showed that the AML^{Inc69} signature,
231 NPM mutation, and WBC count at the time of diagnosis were independent prognostic factors
232 (Figure 4B). C-indices indicated that AML^{Inc69} had better RFS-predictive value than did NPM
233 mutation and WBC count at the time of diagnosis (Supplemental Figure 8). Furthermore,
234 AML^{Inc69} was an independent prognostic factor in the validation cohort, as demonstrated by
235 univariate [hazard ratio (HR), 3.89; 95% confidence interval (CI), 2.04–7.44; $p < 0.001$] and

236 multivariate (HR, 3.56; 95% CI, 1.85–6.84; $p < 0.001$) Cox regression analyses
237 (Supplemental Table 10).

238

239 Based on the multivariate Cox regression analysis results, a nomogram was established using
240 the AML^{inc69}, NPM mutation, and WBC count at the time of diagnosis (Figure 4C). Decision
241 curve analysis indicated that the RFS-predictive effect of the three factors combined was
242 superior to those of the individual factors (Supplemental Figure 9A). AUCs for the prediction
243 of 1-, 2-, and 3-year RFS were 0.76, 0.75, and 0.75, respectively, and the c-index was 0.80
244 (Supplemental Figure 9B). Internal validation yielded a c-index of 0.71 and AUCs for 1-, 2-,
245 and 3-year RFS prediction of 0.76, 0.75, and 0.75, respectively. Calibration curves showed
246 good consistency of these three nomogram predictions with actual observations (Figure 4D).
247 Table 1 provides an overview of all combinations possible and 1-, 2, and 3-year cumulative
248 pedAML relapse risk prediction according to the nomogram. As an example, a patient with
249 pedAML in the AML^{inc69} high-risk group (100 points) with no NPM mutation (60 points) and
250 a WBC count < 50 at the time of diagnosis (0 point) would have a 76.8% cumulative risk of
251 relapse at 3 years.

252

253 **Comparison of characteristics and biological pathway enrichment**

254 Differences in clinical characteristics between the low- and high-risk AML^{inc69} groups were
255 examined (Supplemental Table 11). Relative to the AML^{inc69} low-risk group, the AML^{inc69}
256 high-risk group contained significantly more cases with t(6;11)(q27;q23), t(9;11)(p22;q23),
257 t(10;11)(p11.2;q23), t(11;19)(q23;p13.1), trisomy 21, KMT2A, MRD at the end of courses 1
258 and 2, and HSCT, as well as greater cytogenetic complexity, a younger age at diagnosis, a
259 higher WBC count at the time of diagnosis, and a higher percentage of leukemic bone-
260 marrow blasts (Figure 5).

261

262 To explore the biological pathways associated with the AML^{Inc69} signature, we performed
263 GSEA using the cancer GO, KEGG, and hallmark gene sets. The five most significant results
264 are shown in Supplemental Figure 10, and the clustered pathways are provided in
265 Supplemental Tables 12–14 encompasses all the clustered pathways. The GSEA analysis
266 revealed the significant involvement of the Hedgehog and KRAS pathways and epithelial–
267 mesenchymal transition (EMT) in AML^{Inc69}-based high risk.

268

269 Discussion

270 The survival of patients with pedAML has increased steadily in recent decades, due in large
271 part to the incorporation of risk stratification based on parameters such as cytogenetic and
272 molecular abnormalities and MRD. Currently, pedAML relapse occurs in approximately one-
273 third of patients, which is a major obstacle in treatment and adversely impacts OS^{9,10}. AML
274 relapse is attributable primarily to the poor responsiveness of therapy-resistant leukemic stem
275 cells (LSCs) to common chemotherapeutic agents³⁴. Treatments for pedAML relapse include
276 HSCT and reinduction regimens, but their inevitable generation of side effects remains a
277 challenge⁹.

278

279 No robust prognostic model for the prediction of pedAML relapse is currently available.
280 Several models based on EFS have been developed for pedAML risk stratification. However,
281 due to the inclusion of relapse, induction failure, and death at first event, the LSC6, LSC17,
282 and LSC47 signature and IncScore predicted RFS in the discovery cohort inefficiently.
283 Moreover, we argue that induction failure should be included in analyses as a binary variable,
284 regardless of its temporal span. For these reasons, we excluded induction failure and death,
285 and focused solely on RFS.

286

287 In this study, we demonstrated that the AML^{lnc69} prognostic signature strengthens risk
288 prediction, even in multivariate analysis including established risk-stratifying factors. Among
289 the lncRNAs constituting the signature, MIR100HG (ENSG00000255015)³⁵, MIR17HG
290 (ENSG00000215417)³⁶, MALAT1 (ENSG00000251562)³⁷⁻³⁹, and ZFAS1
291 (ENSG00000177410)⁴⁰⁻⁴³ were previously shown to be associated with AML; the
292 associations of the other 65 lncRNAs with AML are novel. In contrast to the use of median
293 values as dichotomization standards in most studies, we used an outcome-oriented method to
294 identify optimal cutoff values in this study, thereby maximizing the distinction between low-
295 and high-risk groups in terms of RFS. The good RFS-predicting performance of AML^{lnc69}
296 was demonstrated through KM survival plots and ROC curves. Internal validation is crucial
297 for the estimation of a model's generalizability⁴⁴. Compared with other internal validation
298 methods, bootstrap analysis not only enables the use of the entire sample for validation, but
299 also provides nearly unbiased estimates of model performance⁴⁵. The favorable results of
300 bootstrap-based internal validation in this study provide strong evidence for the reliability of
301 model construction. As some high-risk patients underwent HSCT to improve RFS⁴⁶, we split
302 patients in the discovery cohort into HSCT and no-HSCT groups. The model retained its
303 predictive value in both scenarios. Moreover, external validation must be performed to
304 determine a model's reproducibility and generalizability to other samples⁴⁷. Thus, data from
305 the AAML0531 study, distinct from the discovery cohort, was employed for external
306 validation in this study. Although this cohort was small and significantly more heterogeneous
307 than the discovery cohort, the use of the AML^{lnc69} to predict RFS in this cohort was
308 successful. The AUCs obtained in this study were satisfactory, indicating the reproducibility
309 of AML^{lnc69} use in actual practice. The AML^{lnc69} remained predictive independently of
310 gemtuzumab ozogamicin administration in the AAML0531 cohort; no such analysis could be

311 performed for sorafenib or bortezomib administration in the AAML1031 cohort due to the
312 lack of information. With an ever-growing number of pedAML therapeutics available
313 (including bcl-2 protein family and DNA methyltransferase inhibitors), the evaluation of the
314 predictive value of AML^{lnc69} in this evolving therapeutic landscape would be of interest.

315

316 Recently, Farrar et al¹⁴ constructed a lncRNA signature (lncScore) for pedAML with a
317 completely different set of lncRNAs than used in the present study, which might be explained
318 by some notable differences between the studies. First, lncScore was built based on EFS,
319 while AML^{lnc69} was developed using RFS, which thus limits the direct comparison of the
320 performance of both signatures. Second, Farrar et al¹⁴ initially sought to identify lncRNAs
321 that were differentially expressed (DE) in the bone marrow of patients with pedAML and that
322 of healthy individuals to construct a model based on the upregulation of these lncRNAs in
323 pedAML. However, the healthy individuals were actually post-induction patients, whose
324 bone marrow may differ substantially from normal⁴⁸. Third, the selection of DE lncRNAs
325 may have led to the overlooking of some lncRNAs that actually impact prognosis. Thus,
326 instead of performing differential expression analysis, we directly employed the entire
327 lncRNAome for model construction. In addition, Farrar et al¹⁴ constructed a regression model
328 based on EFS, whereas we focused on RFS, and they included samples with low-depth
329 sequencing, whereas we excluded such samples due to the usually low expression of
330 lncRNAs. Despite these differences in composition, construction criteria, and endpoints,
331 however, the two signatures are associated with very similar pathways in GSEAs (data not
332 shown).

333

334 Surprisingly, the standard-risk group (as defined in the TARGET cohort based on cytogenic
335 and molecular characteristics) had worse RFS than did the high-risk group. Aplenc et al.²⁶

336 reported that approximately 78% of patients in the AAML1031 study were allocated to the
337 low-risk group, with the remainder allocated to the high-risk group. However, a large number
338 of these patients were reassigned to the standard-risk group in the TARGET database with the
339 application of additional cytogenetic and molecular risk stratification criteria. In addition,
340 ‘AML^{lnc69}-Low_Risk group-High’ patients, the majority of whom underwent HSCT, had
341 better RFS than did ‘AML^{lnc69}-Low_Risk group-Low/Standard’ patients in this study. A
342 portion of patients that were initially classified as ‘Risk group-Low/Standard’, missing HSCT,
343 would have been reclassified as high risk, potentially explaining the superior RFS in
344 ‘AML^{lnc69}-Low_Risk group-High’ patients relative to that of patients in the other two groups.
345 Due to the retrospective nature of this study and the complexity of evolving risk stratification,
346 however, complete clarification of these observed differences is difficult. Nevertheless, the
347 results clearly suggest that all stratification schemes, including that used in the AAML1031
348 study and traditional cytogenetic and molecular risk stratification, have limitations resulting
349 in the under- or overestimation of the pedAML relapse risk. Importantly, the AML^{lnc69}
350 successfully stratified patients in the three TARGET risk groups (low, standard, and high)
351 based on their RFS.

352

353 The AML^{lnc69} was shown to be an independent predictor of RFS in the discovery and
354 validation cohorts. With the continued undertaking of large -omics studies and identification
355 of novel risk-stratifying parameters, such as UBTF-TD⁴⁹ and GLIS2-fusions^{50,51}, the
356 assessment of the predictive value of AML^{lnc69} in prospective clinical studies^{52,53}
357 documenting those molecular aberrations would be of great interest. Based on the results of
358 the multivariate Cox regression analysis of discovery cohort data, we developed a nomogram
359 for the intuitive prediction of the RFS of patients with pedAML that includes the AML^{lnc69},
360 NPM mutation, and WBC count at the time of diagnosis. Relative to the isolated application

361 of each factor, the nomogram provides for more-refined estimation of 1-, 2-, and 3-year
362 cumulative relapse risks. With further independent validation, this tool could offer valuable
363 insights for prognostic assessment and therapeutic decision making in the clinical context.

364

365 The GSEA performed in this study revealed that Hedgehog- and KRAS-associated pathways
366 and EMT played important roles in the AML^{lnc69}-based estimation of high relapse risk. The
367 Hedgehog signaling pathway plays a fundamental role in LSC quiescence and may be an
368 effective target for the prevention of pedAML relapse^{54,55}. Similarly, KRAS contributes to the
369 emergence of stemness traits⁵⁶, and KRAS mutations are frequent in patients with pedAML
370 and associated with worse outcomes⁵⁷⁻⁵⁹. EMT is a well-known cellular program that is
371 crucial for the relapse and metastasis of various tumors, and it plays a key role in the
372 progression and relapse of AML⁶⁰⁻⁶².

373

374 In conclusion, we generated a comprehensive prognostic model including 69 lncRNAs for the
375 prediction of the RFS of patients with pedAML. To our knowledge, this study was the first
376 comprehensive evaluation of relationships between lncRNAs and RFS in this population. We
377 provide evidence that our model could further refine current risk stratification. Its application
378 requires the design of a microarray or targeted RNA sequencing panel, which is currently the
379 standard of practice in many clinical laboratories handling oncological diagnosis⁶³. Although
380 the AML^{lnc69} is associated with several known predictive markers, it incorporates more
381 information than provided by these individual factors. Thus, AML^{lnc69} use may avoid the
382 need to perform numerous molecular and cellular assays, as is currently done for the full risk
383 classification of patients with pedAML, and thereby be a great asset in resource-limited
384 circumstances. Furthermore, samples from patients' bone marrow or peripheral blood,
385 routinely collected during standard pedAML diagnosis, can be used. This lack of need for

386 additional sample collection makes this method straightforward, cost effective, and easily
387 implementable. Further validation of the AML^{Inc69} with large independent cohorts is needed
388 to definitively confirm its clinical value.

389

390 **Contributions**

391 Z.R, J.V, and T.L drafted the manuscript. Z.R, J.V and T.L designed the figures. All authors
392 critically revised the manuscript and approved the final version.

393 None of the authors has a relevant conflict of interest.

394 **References**

- 395 1. Zwaan CM, Kolb EA, Reinhardt D, et al. Collaborative Efforts Driving Progress in
396 Pediatric Acute Myeloid Leukemia. *J Clin Oncol.* 2015;33(27):2949-2962.
- 397 2. Elgarten CW, Aplenc R. Pediatric acute myeloid leukemia: updates on biology, risk
398 stratification, and therapy. *Current Opinion in Pediatrics.* 2020;32(1):57-66.
- 399 3. Shiba N. Comprehensive molecular understanding of pediatric acute myeloid
400 leukemia. *Int J Hematol.* 2023;117(2):173-181.
- 401 4. de Rooij JD, Zwaan CM, van den Heuvel-Eibrink M. Pediatric AML: From Biology
402 to Clinical Management. *J Clin Med.* 2015;4(1):127-149.
- 403 5. Creutzig U, Zimmermann M, Reinhardt D, et al. Changes in cytogenetics and
404 molecular genetics in acute myeloid leukemia from childhood to adult age groups. *Cancer.*
405 2016;122(24):3821-3830.
- 406 6. Loken MR, Alonzo TA, Pardo L, et al. Residual disease detected by multidimensional
407 flow cytometry signifies high relapse risk in patients with de novo acute myeloid leukemia: a
408 report from Children's Oncology Group. *Blood.* 2012;120(8):1581-1588.
- 409 7. Schuurhuis GJ, Heuser M, Freeman S, et al. Minimal/measurable residual disease in
410 AML: a consensus document from the European LeukemiaNet MRD Working Party. *Blood.*
411 2018;131(12):1275-1291.
- 412 8. Tierens A, Bjorklund E, Siitonen S, et al. Residual disease detected by flow cytometry
413 is an independent predictor of survival in childhood acute myeloid leukaemia; results of the
414 NOPHO-AML 2004 study. *Br J Haematol.* 2016;174(4):600-609.
- 415 9. Egan G, Tasian SK. Relapsed pediatric acute myeloid leukaemia: state-of-the-art in
416 2023. *Haematologica.* 2023;108(9):2275-2288.
- 417 10. Hoffman AE, Schoonmade LJ, Kaspers GJ. Pediatric relapsed acute myeloid
418 leukemia: a systematic review. *Expert Rev Anticancer Ther.* 2021;21(1):45-52.
- 419 11. Elsayed AH, Rafiee R, Cao X, et al. A six-gene leukemic stem cell score identifies
420 high risk pediatric acute myeloid leukemia. *Leukemia.* 2020;34(3):735-745.
- 421 12. Duployez N, Marceau-Renaut A, Villenet C, et al. The stem cell-associated gene
422 expression signature allows risk stratification in pediatric acute myeloid leukemia. *Leukemia.*
423 2019;33(2):348-357.
- 424 13. Huang BJ, Smith JL, Farrar JE, et al. Integrated stem cell signature and cytomolecular
425 risk determination in pediatric acute myeloid leukemia. *Nat Commun.* 2022;13(1):5487.
- 426 14. Farrar JE, Smith JL, Othus M, et al. Long Noncoding RNA Expression Independently
427 Predicts Outcome in Pediatric Acute Myeloid Leukemia. *J Clin Oncol.* 2023;JCO2201114.
- 428 15. Fatica A, Bozzoni I. Long non-coding RNAs: new players in cell differentiation and
429 development. *Nat Rev Genet.* 2014;15(1):7-21.
- 430 16. Esteller M. Non-coding RNAs in human disease. *Nature Reviews Genetics.*
431 2011;12(12):861-874.
- 432 17. Batista PJ, Chang HY. Long Noncoding RNAs: Cellular Address Codes in
433 Development and Disease. *Cell.* 2013;152(6):1298-1307.
- 434 18. Neyazi S, Ng M, Heckl D, Klusmann JH. Long noncoding RNAs as regulators of
435 pediatric acute myeloid leukemia. *Mol Cell Pediatr.* 2022;9(1):10.
- 436 19. Delas MJ, Sabin LR, Dolzhenko E, et al. lncRNA requirements for mouse acute
437 myeloid leukemia and normal differentiation. *Elife.* 2017;6.
- 438 20. Nobili L, Lionetti M, Neri A. Long non-coding RNAs in normal and malignant
439 hematopoiesis. *Oncotarget.* 2016;7(31):50666-50681.
- 440 21. Garzon R, Volinia S, Papaioannou D, et al. Expression and prognostic impact of
441 lncRNAs in acute myeloid leukemia. *Proceedings of the National Academy of Sciences of the*
442 *United States of America.* 2014;111(52):18679-18684.

- 443 22. Liu DX. Identification of a prognostic lncRNA signature for ER-positive, ER-
444 negative and triple-negative breast cancers. *Breast Cancer Research and Treatment*.
445 2020;183(1):95-105.
- 446 23. Sathipati SY, Sahu D, Huang HC, Lin YC, Ho SY. Identification and characterization
447 of the lncRNA signature associated with overall survival in patients with neuroblastoma.
448 *Scientific Reports*. 2019;9.
- 449 24. Gamis AS, Alonzo TA, Meshinchi S, et al. Gemtuzumab ozogamicin in children and
450 adolescents with de novo acute myeloid leukemia improves event-free survival by reducing
451 relapse risk: results from the randomized phase III Children's Oncology Group trial
452 AAML0531. *J Clin Oncol*. 2014;32(27):3021-3032.
- 453 25. Pollard JA, Alonzo TA, Gerbing R, et al. Sorafenib in Combination With Standard
454 Chemotherapy for Children With High Allelic Ratio FLT3/ITD+ Acute Myeloid Leukemia:
455 A Report From the Children's Oncology Group Protocol AAML1031. *J Clin Oncol*.
456 2022;40(18):2023-2035.
- 457 26. Aplenc R, Meshinchi S, Sung L, et al. Bortezomib with standard chemotherapy for
458 children with acute myeloid leukemia does not improve treatment outcomes: a report from
459 the Children's Oncology Group. *Haematologica*. 2020;105(7):1879-1886.
- 460 27. Cunningham F, Allen JE, Allen J, et al. Ensembl 2022. *Nucleic Acids Res*.
461 2022;50(D1):D988-D995.
- 462 28. Harrell FE, Jr., Lee KL, Mark DB. Multivariable prognostic models: issues in
463 developing models, evaluating assumptions and adequacy, and measuring and reducing errors.
464 *Stat Med*. 1996;15(4):361-387.
- 465 29. Efron B. 1977 RIETZ LECTURE - BOOTSTRAP METHODS - ANOTHER LOOK
466 AT THE JACKKNIFE. *Annals of Statistics*. 1979;7(1):1-26.
- 467 30. Steyerberg EW, Harrell FE, Jr. Prediction models need appropriate internal, internal-
468 external, and external validation. *J Clin Epidemiol*. 2016;69:245-247.
- 469 31. Balachandran VP, Gonen M, Smith JJ, DeMatteo RP. Nomograms in oncology: more
470 than meets the eye. *Lancet Oncol*. 2015;16(4):e173-180.
- 471 32. Subramanian A, Tamayo P, Mootha VK, et al. Gene set enrichment analysis: a
472 knowledge-based approach for interpreting genome-wide expression profiles. *Proc Natl Acad*
473 *Sci U S A*. 2005;102(43):15545-15550.
- 474 33. Liberzon A, Subramanian A, Pinchback R, Thorvaldsdottir H, Tamayo P, Mesirov JP.
475 Molecular signatures database (MSigDB) 3.0. *Bioinformatics*. 2011;27(12):1739-1740.
- 476 34. Stelmach P, Trumpp A. Leukemic stem cells and therapy resistance in acute myeloid
477 leukemia. *Haematologica*. 2023;108(2):353-366.
- 478 35. Emmrich S, Streltsov A, Schmidt F, Thangapandi VR, Reinhardt D, Klusmann JH.
479 LincRNAs MONC and MIR100HG act as oncogenes in acute megakaryoblastic leukemia.
480 *Mol Cancer*. 2014;13:171.
- 481 36. Yan J, Yao L, Li P, Wu G, Lv X. Long non-coding RNA MIR17HG sponges
482 microRNA-21 to upregulate PTEN and regulate homoharringtonine-based chemoresistance
483 of acute myeloid leukemia cells. *Oncol Lett*. 2022;23(1):24.
- 484 37. Jin J, Fu L, Hong P, Feng W. MALAT-1 regulates the AML progression by
485 promoting the m6A modification of ZEB1. *Acta Biochim Pol*. 2023;70(1):37-43.
- 486 38. Sheng XF, Hong LL, Li H, Huang FY, Wen Q, Zhuang HF. Long non-coding RNA
487 MALAT1 modulate cell migration, proliferation and apoptosis by sponging microRNA-146a
488 to regulate CXCR4 expression in acute myeloid leukemia. *Hematology*. 2021;26(1):43-52.
- 489 39. Hu N, Chen L, Wang C, Zhao H. MALAT1 knockdown inhibits proliferation and
490 enhances cytarabine chemosensitivity by upregulating miR-96 in acute myeloid leukemia
491 cells. *Biomed Pharmacother*. 2019;112:108720.

- 492 40. Su L, Kong H, Wu F, et al. Long non-coding RNA zinc finger antisense 1 functions as
493 an oncogene in acute promyelocytic leukemia cells. *Oncol Lett.* 2019;18(6):6331-6338.
- 494 41. Guo H, Wu L, Zhao P, Feng A. Overexpression of long non-coding RNA zinc finger
495 antisense 1 in acute myeloid leukemia cell lines influences cell growth and apoptosis. *Exp*
496 *Ther Med.* 2017;14(1):647-651.
- 497 42. Li Q, Wang J. Long noncoding RNA ZFAS1 enhances adriamycin resistance in
498 pediatric acute myeloid leukemia through the miR-195/Myb axis. *RSC Adv.*
499 2019;9(48):28126-28134.
- 500 43. Gan S, Ma P, Ma J, et al. Knockdown of ZFAS1 suppresses the progression of acute
501 myeloid leukemia by regulating microRNA-150/Sp1 and microRNA-150/Myb pathways. *Eur*
502 *J Pharmacol.* 2019;844:38-48.
- 503 44. Steyerberg EW. Clinical Prediction Models: A Practical Approach to
504 Development, Validation, and Updating.: New York: Springer; 2019.
- 505 45. Harrell FE, Jr. Regression Modeling Strategies: With Applications to Linear
506 Models, Logistic Regression, and Survival Analysis, 2nd Edition. : New York: Springer;
507 2015.
- 508 46. Cooper TM, Ries RE, Alonzo TA, et al. Revised Risk Stratification Criteria for
509 Children with Newly Diagnosed Acute Myeloid Leukemia: A Report from the Children's
510 Oncology Group. *Blood.* 2017;130.
- 511 47. Ramspek CL, Jager KJ, Dekker FW, Zoccali C, van Diepen M. External validation of
512 prognostic models: what, why, how, when and where? *Clin Kidney J.* 2021;14(1):49-58.
- 513 48. dbGap. TARGET: Acute Myeloid Leukemia (AML). dbGaP Study Accession:
514 phs000465v19p8. [https://www.ncbi.nlm.nih.gov/projects/gap/cgi-](https://www.ncbi.nlm.nih.gov/projects/gap/cgi-bin/study.cgi?study_id=phs000465.v19.p8)
515 [bin/study.cgi?study_id=phs000465.v19.p8](https://www.ncbi.nlm.nih.gov/projects/gap/cgi-bin/study.cgi?study_id=phs000465.v19.p8)
- 516 49. Umeda M, Ma J, Huang BJ, et al. Integrated Genomic Analysis Identifies UBTF
517 Tandem Duplications as a Recurrent Lesion in Pediatric Acute Myeloid Leukemia. *Blood*
518 *Cancer Discov.* 2022;3(3):194-207.
- 519 50. Conneely SE, Stevens AM. Acute Myeloid Leukemia in Children: Emerging
520 Paradigms in Genetics and New Approaches to Therapy. *Curr Oncol Rep.* 2021;23(2):16.
- 521 51. Aid Z, Robert E, Lopez CK, et al. High caspase 3 and vulnerability to dual BCL2
522 family inhibition define ETO2::GLIS2 pediatric leukemia. *Leukemia.* 2023;37(3):571-579.
- 523 52. Karlsson L, Cheuk D, De Moerloose B, et al. Characteristics and outcome of primary
524 resistant disease in paediatric acute myeloid leukaemia. *Br J Haematol.* 2023;201(4):757-765.
- 525 53. Kaspers GJL, Wijnen NE, Koedijk JB, et al. Chip-AML22 Master Protocol: An Open-
526 Label Clinical Trial in Newly Diagnosed Pediatric De Novo Acute Myeloid Leukemia (AML)
527 Patients Including a Linked Phase II Trial with Quizartinib in FLT3-ITD/ NPM1wt Patients -
528 a Study By the NOPHO-DB-SHIP Consortium. *Blood.* 2023;142(Supplement 1):1532-1532.
- 529 54. Pession A, Lonetti A, Bertuccio S, Locatelli F, Masetti R. Targeting Hedgehog
530 pathway in pediatric acute myeloid leukemia: challenges and opportunities. *Expert Opin Ther*
531 *Targets.* 2019;23(2):87-91.
- 532 55. Lainez-Gonzalez D, Serrano-Lopez J, Alonso-Dominguez JM. Understanding the
533 Hedgehog Signaling Pathway in Acute Myeloid Leukemia Stem Cells: A Necessary Step
534 toward a Cure. *Biology (Basel).* 2021;10(4).
- 535 56. Chippalkatti R, Abankwa D. Promotion of cancer cell stemness by Ras. *Biochem Soc*
536 *Trans.* 2021;49(1):467-476.
- 537 57. Bolouri H, Farrar JE, Triche T, Jr., et al. The molecular landscape of pediatric acute
538 myeloid leukemia reveals recurrent structural alterations and age-specific mutational
539 interactions. *Nat Med.* 2018;24(1):103-112.

- 540 58. Mustafa Ali MK, Williams MT, Corley EM, AlKaabba F, Niyongere S. Impact of
541 KRAS and NRAS mutations on outcomes in acute myeloid leukemia. *Leuk Lymphoma*.
542 2023;64(5):962-971.
- 543 59. Ball BJ, Hsu M, Devlin SM, et al. The prognosis and durable clearance of RAS
544 mutations in patients with acute myeloid leukemia receiving induction chemotherapy. *Am J*
545 *Hematol*. 2021;96(5):E171-E175.
- 546 60. Dongre A, Weinberg RA. New insights into the mechanisms of epithelial-
547 mesenchymal transition and implications for cancer. *Nat Rev Mol Cell Biol*. 2019;20(2):69-
548 84.
- 549 61. Chen SC, Liao TT, Yang MH. Emerging roles of epithelial-mesenchymal transition in
550 hematological malignancies. *J Biomed Sci*. 2018;25(1):37.
- 551 62. Carmichael CL, Wang J, Nguyen T, et al. The EMT modulator SNAI1 contributes to
552 AML pathogenesis via its interaction with LSD1. *Blood*. 2020;136(8):957-973.
- 553 63. Tiwari M. Microarrays and cancer diagnosis. *J Cancer Res Ther*. 2012;8(1):3-10.
554

555

556

557

558

559

560

561

562

563

564

565

566

567

568

569

570

571

572 **Figure legends**

573

574 **Figure 1. Identification of the 69 relapse-related lncRNAs prognostic signature for**
575 **pedAML patients.** (A) Coefficients of the 69 lncRNAs originated from the LASSO Cox
576 regression. (B) Risk score distribution and RFS status map of pedAML patients. lncRNA,
577 long non-coding RNA; LASSO, least absolute shrinkage and selection operator; RFS,
578 relapse-free survival; pedAML, pediatric acute myeloid leukemia.

579

580 **Figure 2. Validation of AML^{lnc69}.** (A, B) Kaplan–Meier survival curve of pedAML patients’
581 RFS (A) and OS (B) in the low- and high-risk groups. (C) ROC curves and AUCs for 1-, 2-,
582 and 3-year RFS. PedAML, pediatric acute myeloid leukemia; RFS, relapse-free survival; OS,
583 overall survival; ROC, receiver operating characteristic; AUC, area under the curve.

584

585 **Figure 3. The performance of AML^{lnc69} in terms of whether or not undergoing HSCT in**
586 **1st CR and cytogenetic/molecular risk.** (A, B) Kaplan–Meier survival curves of RFS for
587 the pedAML patients receiving HSCT (A) and without receiving HSCT in the first CR (B).
588 (C) The distribution of cytogenetic/molecular risk between low- and high-risk groups based
589 on AML^{lnc69}. (D-F) Kaplan–Meier survival curve of pedAML patients' RFS based on
590 AML^{lnc69} in low-, standard- and high-risk groups categorized by cytogenetic/molecular risk
591 stratification. HSCT, hematopoietic stem cell transplantation; CR, complete remission;
592 pedAML, pediatric acute myeloid leukemia; RFS, relapse-free survival.

593

594 **Figure 4. Independent prognostic analysis of AML^{lnc69}.** (A, B) Forest plots of univariate (A)
595 and multivariate (B) independent Cox regression analyses of AML^{lnc46} and other characters.
596 (C) Nomogram model of the combined AML^{lnc46}, NPM mutation and WBC at diagnosis for
597 1-, 2-, and 3-year relapse risk in pedAML patients. (D) Calibration plot comparing
598 nomogram-predicted and actual RFS at 1-, 2-, and 3-year. PedAML, pediatric acute myeloid
599 leukemia; RFS, relapse-free survival.

600

601 **Figure 5. Comparison of significant characters between AML^{lnc69} low- and high-risk**
602 **groups.** (A) Heatmap comparing the distribution of significant characters. (B-D)
603 Comparison of age (B), WBC at diagnosis (C) and bone marrow leukemic blast (D). WBC,
604 white blood cell.

605 **Tables**

606

607 **TABLE 1 Examples of 1-, 2-, and 3-year relapse risk prediction for pedAML patients**

608 **using the nomogram prediction model.**

609

AML^{Inc69}	NPM mutation	WBC at diagnosis	1-Year Risk, % (95% CI)	2-Year Risk, % (95% CI)	3-Year Risk, % (95% CI)
High	No	≥50	56.8 (48.3-63.8)	80.5 (72.9-86.0)	83.6 (76.4-88.7)
High	Yes	≥50	29.8 (14.2-42.6)	49.9 (26.1-66.0)	53.4 (28.5-69.7)
High	No	<50	49.2 (42.1-55.5)	73.3 (66.1-79.0)	76.8 (69.8-82.2)
High	Yes	<50	24.9 (11.7-36.2)	42.8 (21.7-58.2)	46.1 (23.8-61.9)
Low	No	≥50	18.1 (13.8-22.3)	32.3 (25.6-38.4)	35.1 (28.0-41.4)
Low	Yes	≥50	8.1 (3.7-12.4)	15.2 (7.2-22.5)	16.7 (7.9-24.6)
Low	No	<50	14.9 (11.9-17.9)	27.1 (22.5-31.4)	29.5 (24.7-34.0)
Low	Yes	<50	6.6 (3.0-10.0)	12.5 (6.0-18.5)	13.7 (6.6-20.3)

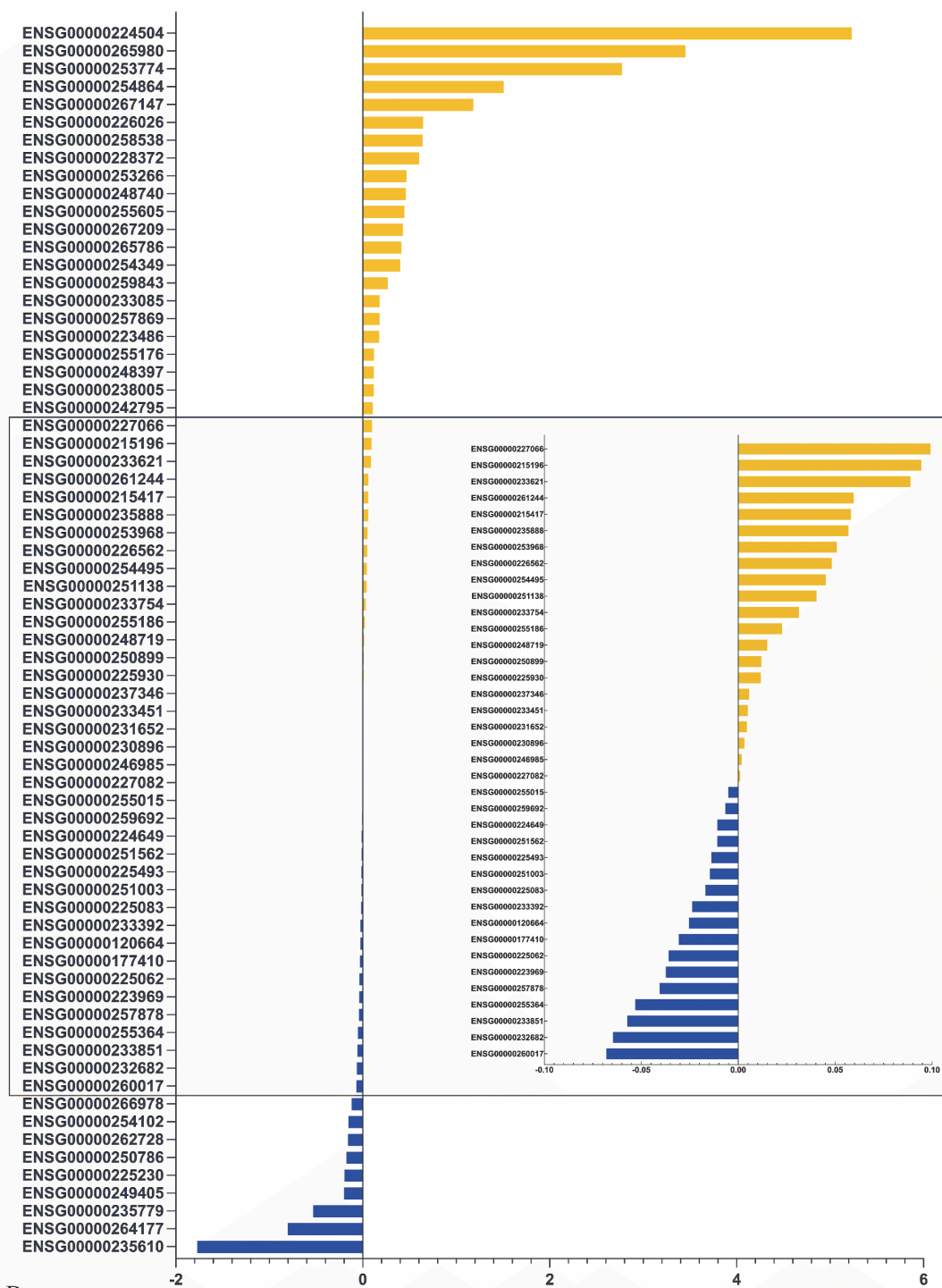
610

611 Abbreviations: WBC: white blood cell.

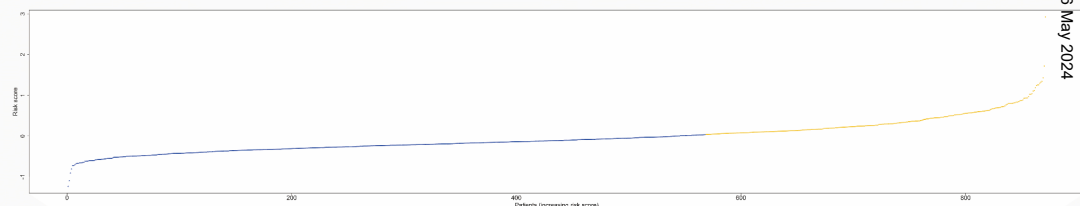
612

Figure 1

A



B



C

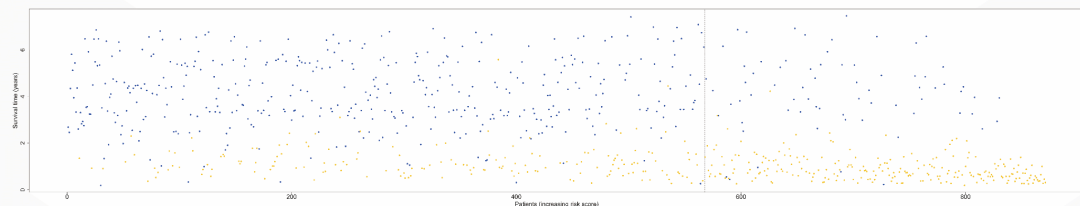


Figure 2

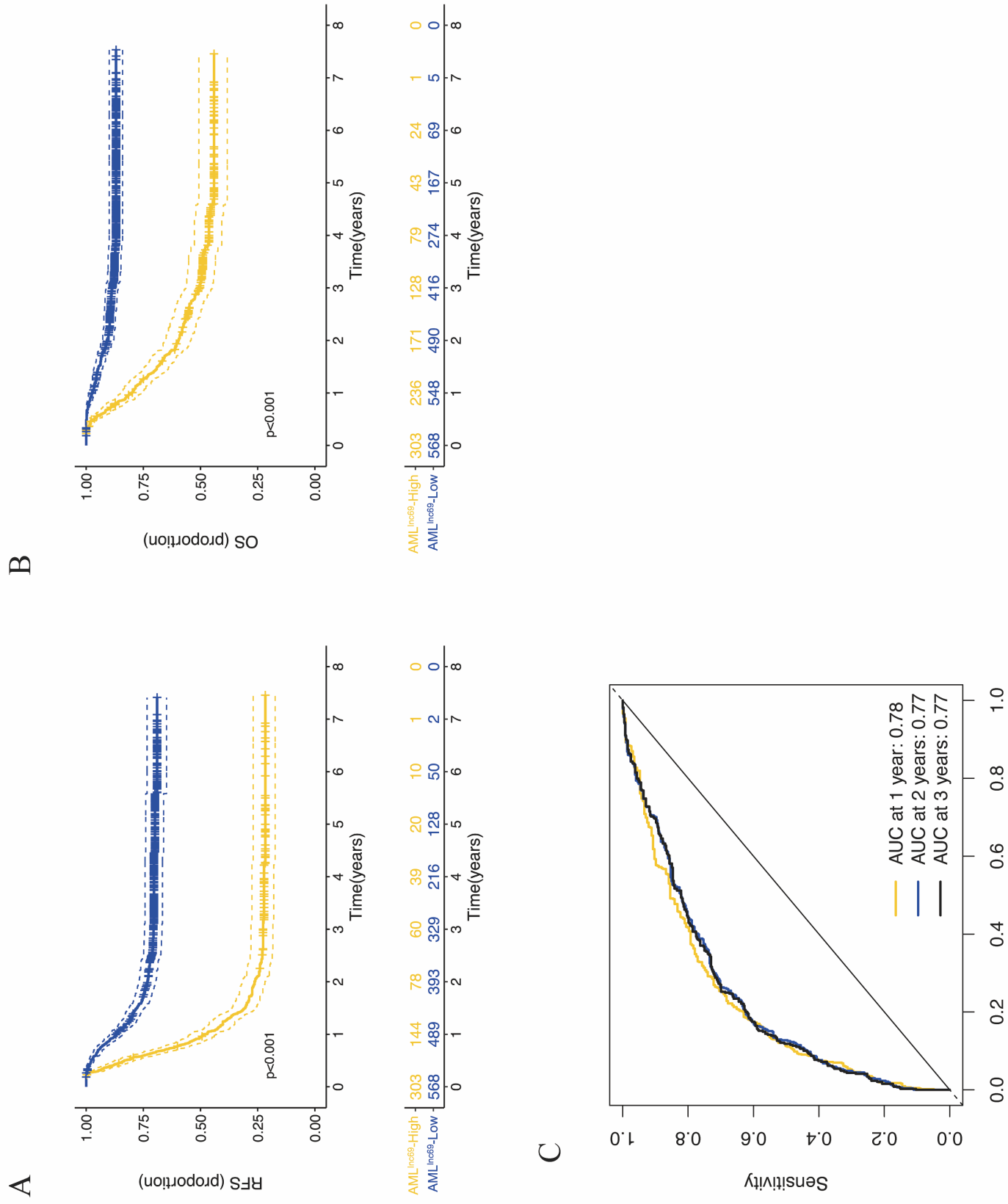
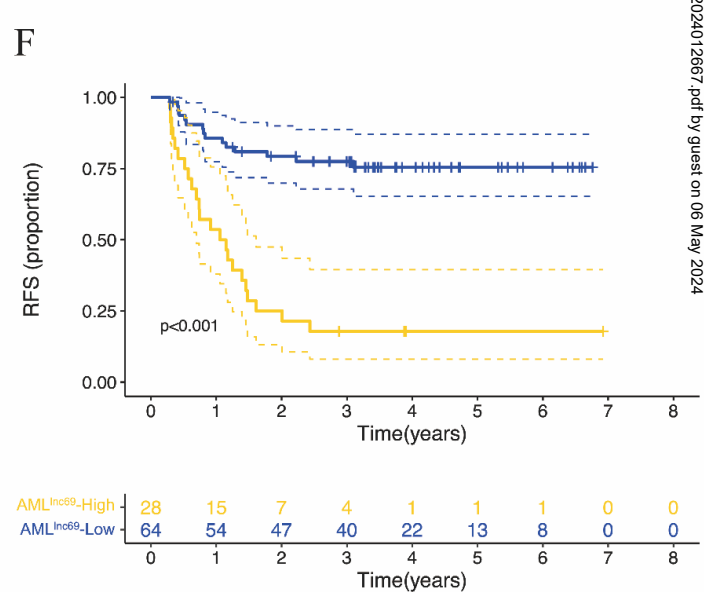
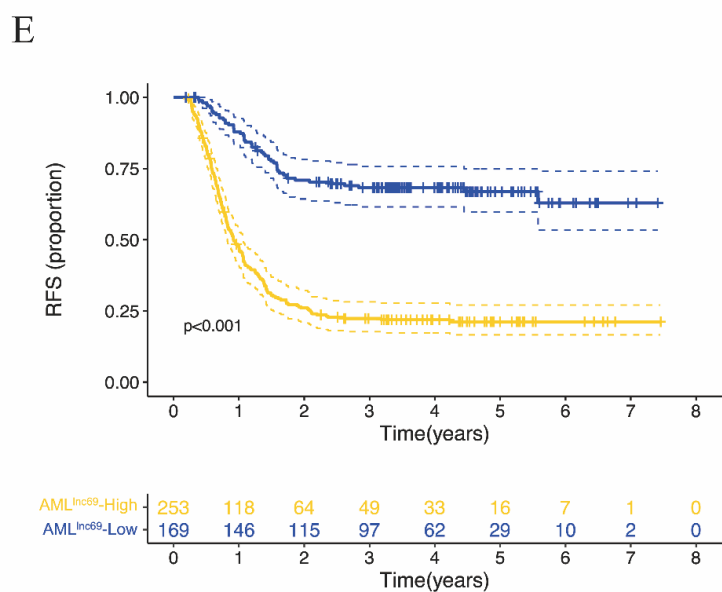
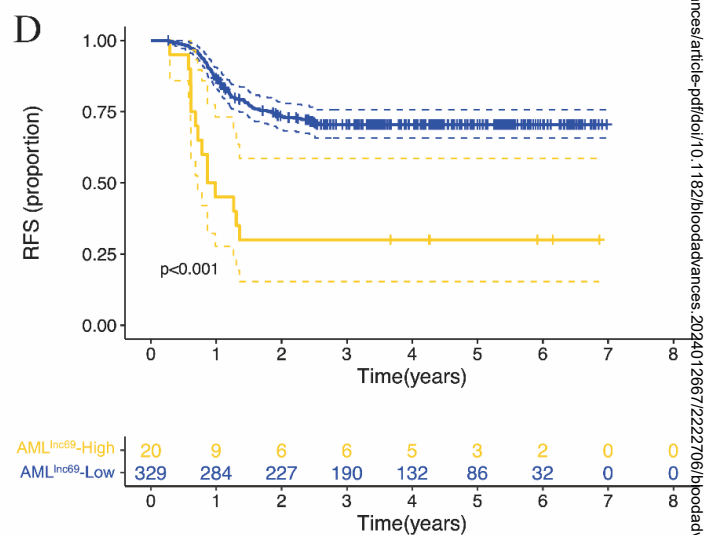
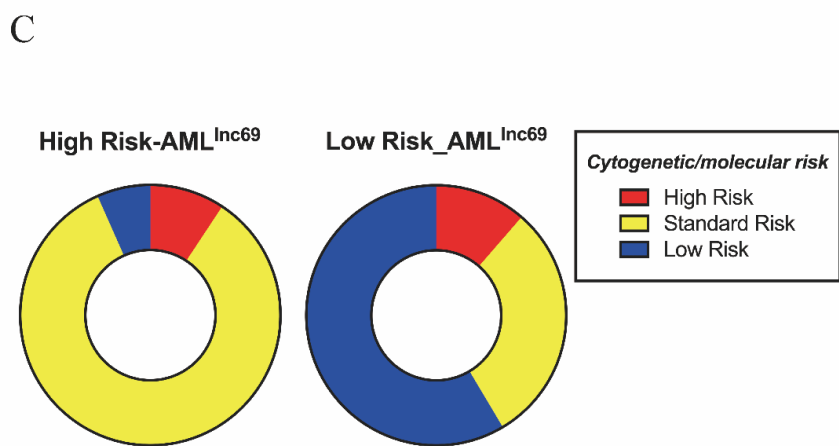
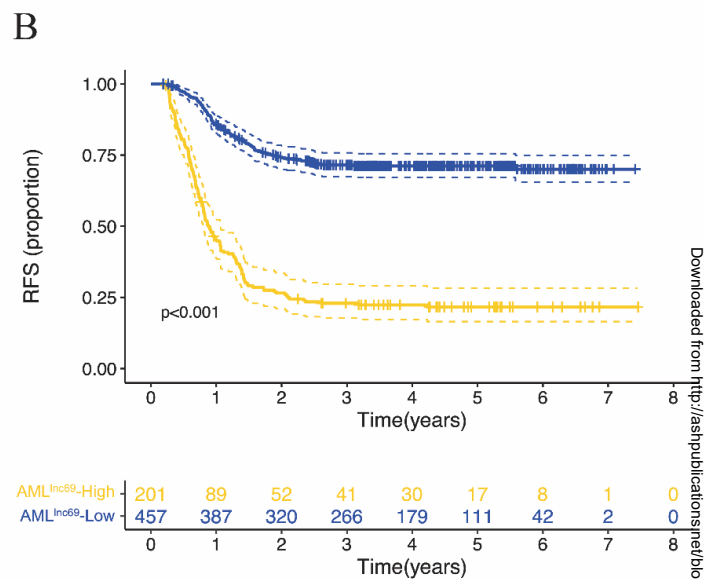
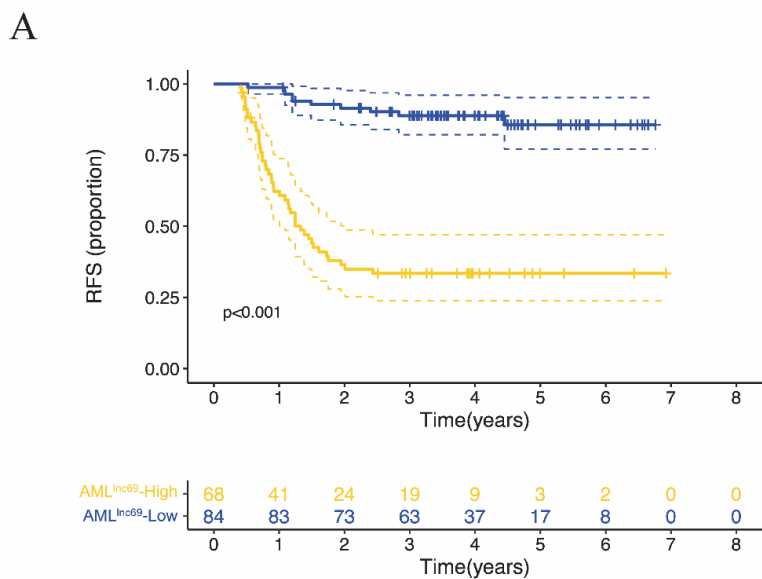
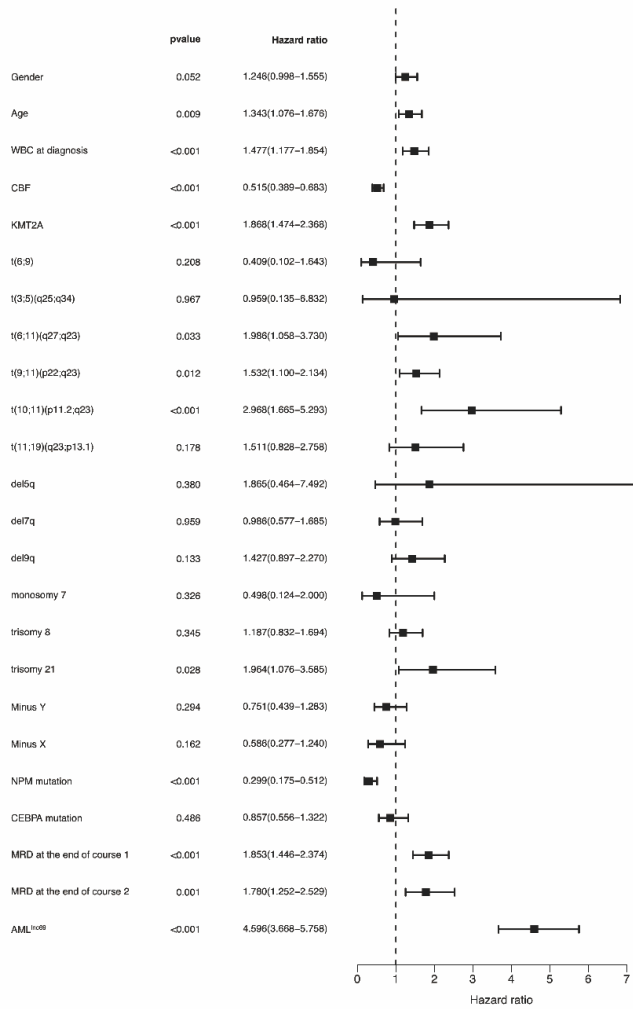


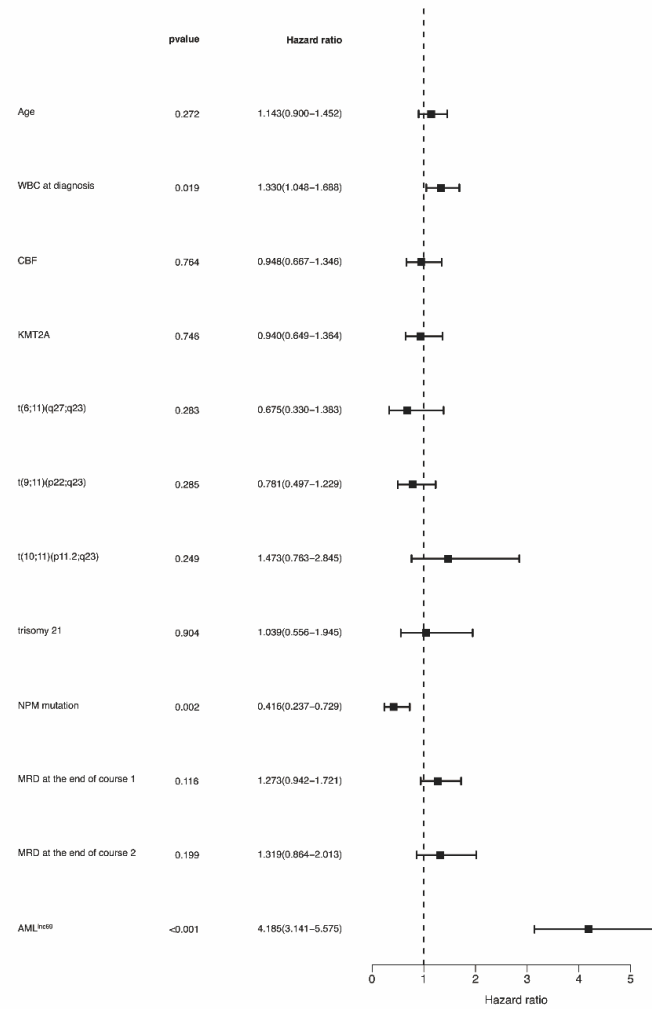
Figure 3



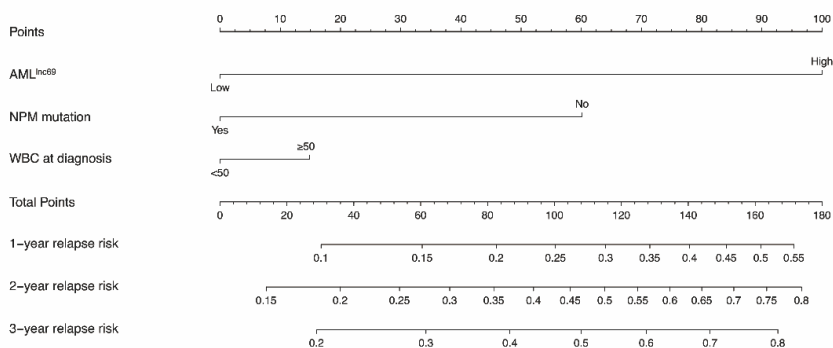
A



B



C



D

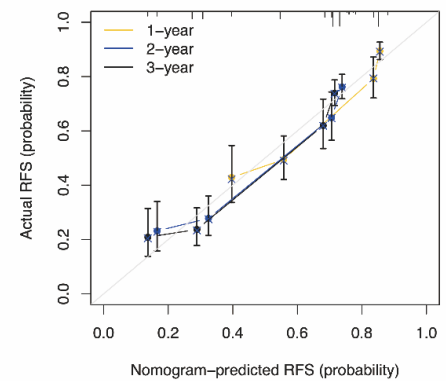
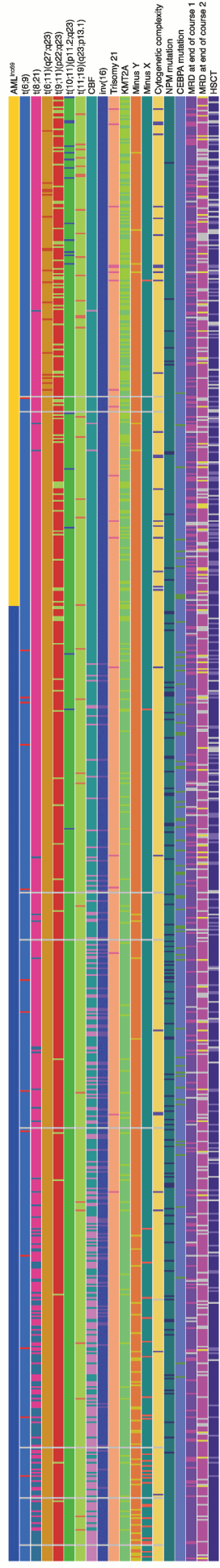
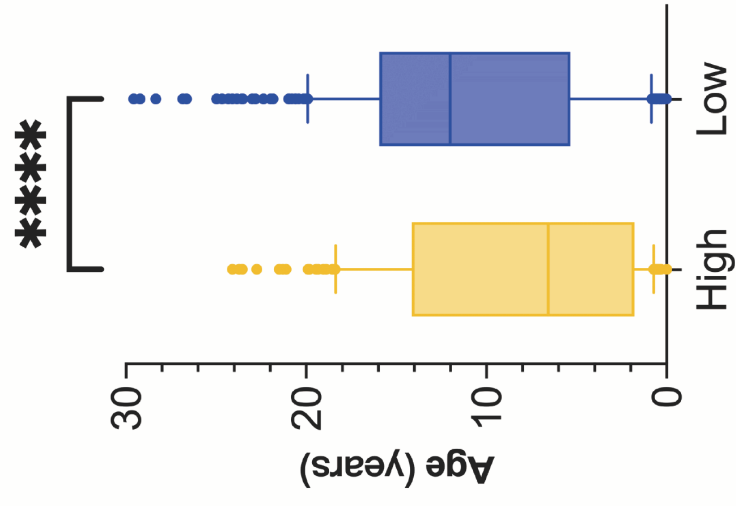


Figure 5

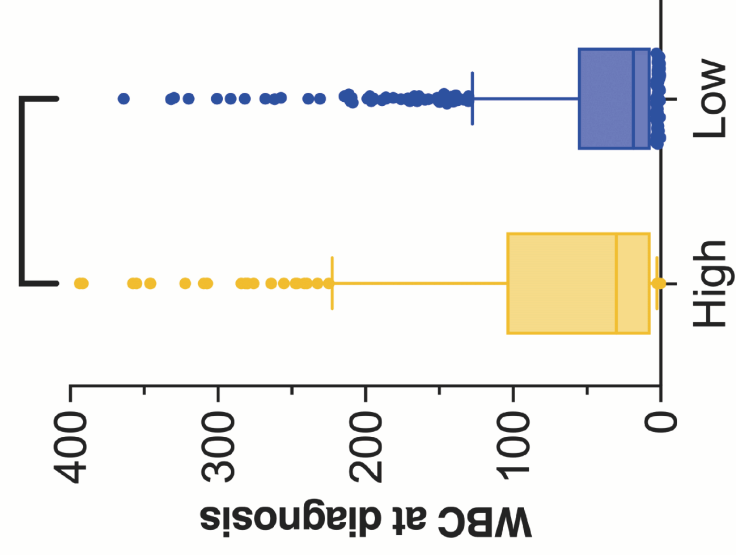
A



B



C



D

